

Exploring Meson Structure via Lattice QCD

Qi Shi

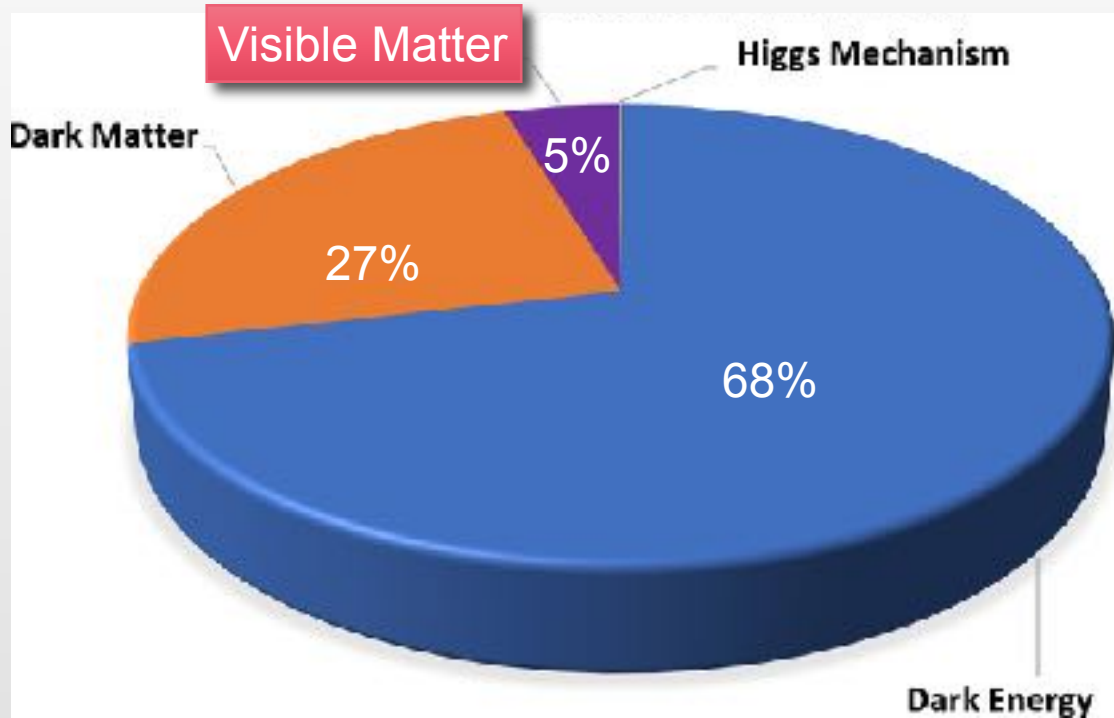
In collaboration with H.-T. Ding, X. Gao, A.D. Hanlon, S. Mukherjee, P. Petreczky, S. Syritsyn, R. Zhang and Y. Zhao

CONTENTS

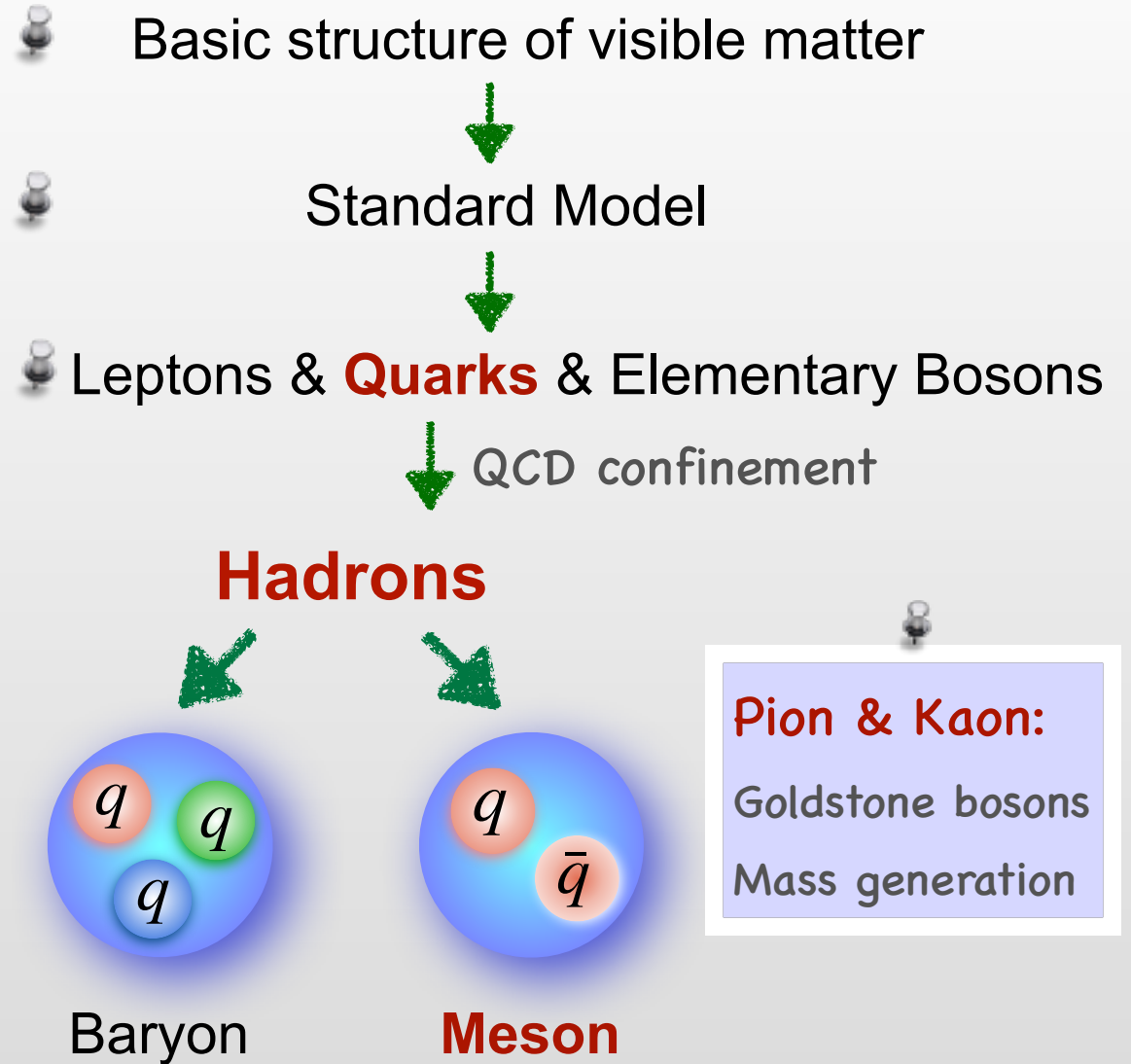
- 1 Background and Motivation
- 2 Lattice QCD Methodology
- 3 Hadron Structure:
 - ★ Electromagnetic Form Factors (EMFFs)
 - Based on *Phys. Rev. Lett.* 133 (2024) 18, 181902
 - ★ Generalized Parton Distributions (GPDs)
 - Based on *JHEP*, 02 (2025) 056
- 4 Conclusion

Introduction

Front. Phys. 16 (2021) 6, 64701



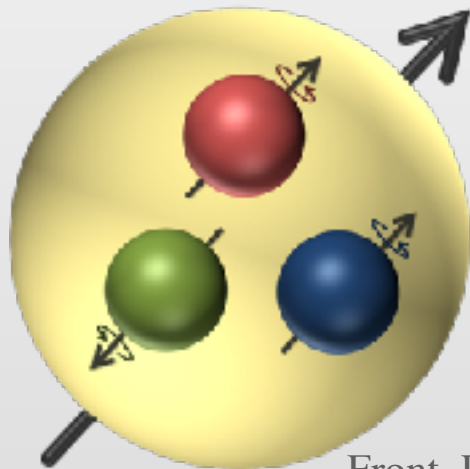
Mass-energy budget of the universe



Hadron Structure

📌 Naive quark model

only valence quarks



Front. Phys. 16 (2021) 6, 64701

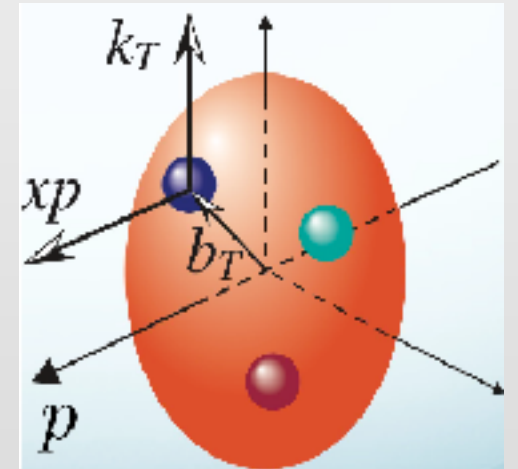
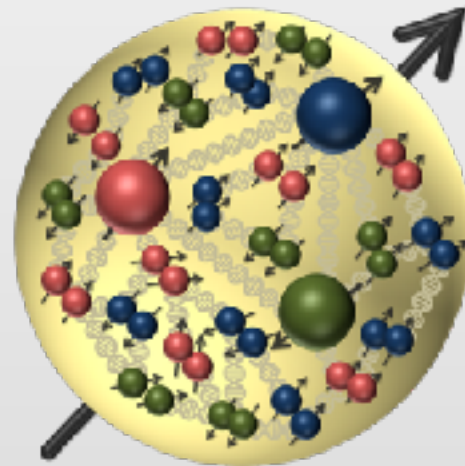
DIS experiments



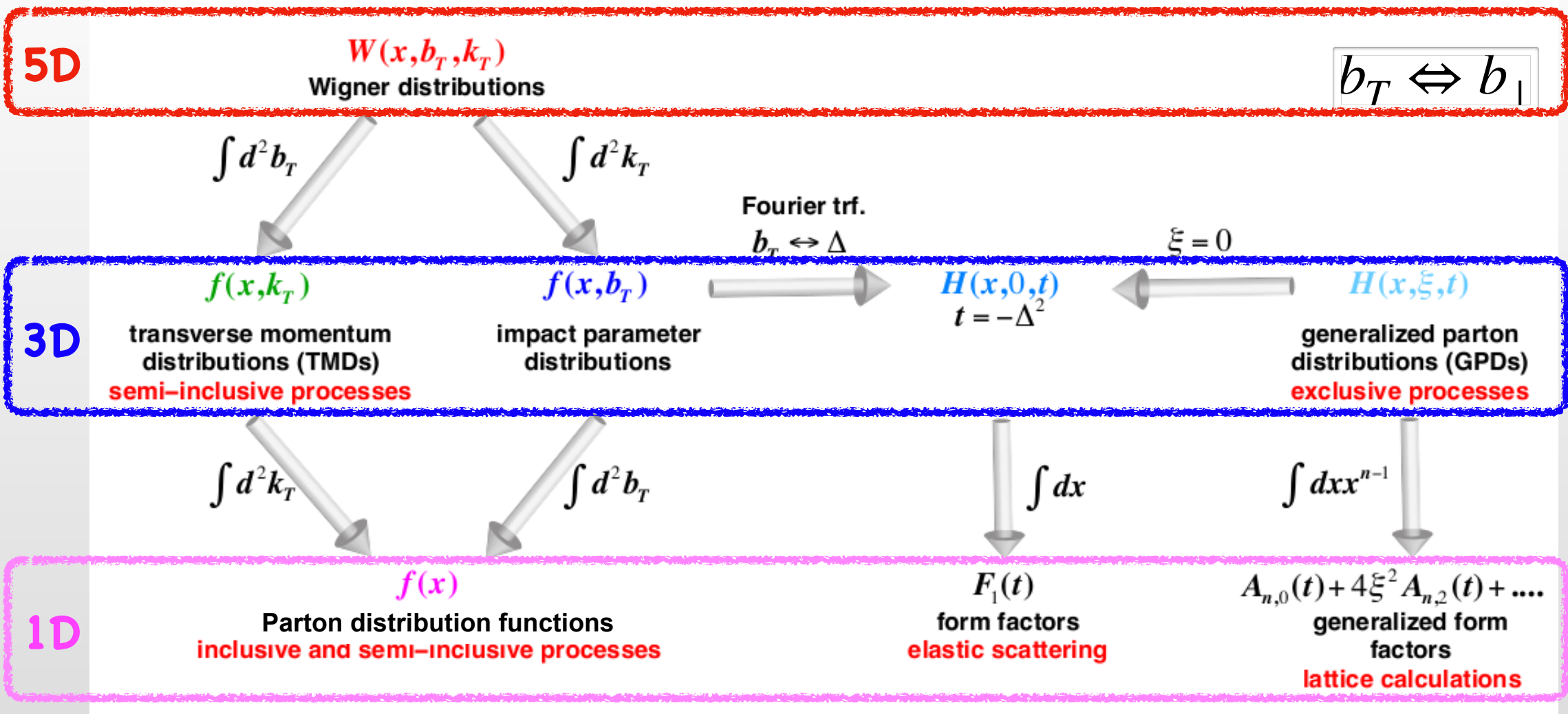
📌 Modern quark model

valence quarks +
see quark-antiquark pairs + gluons

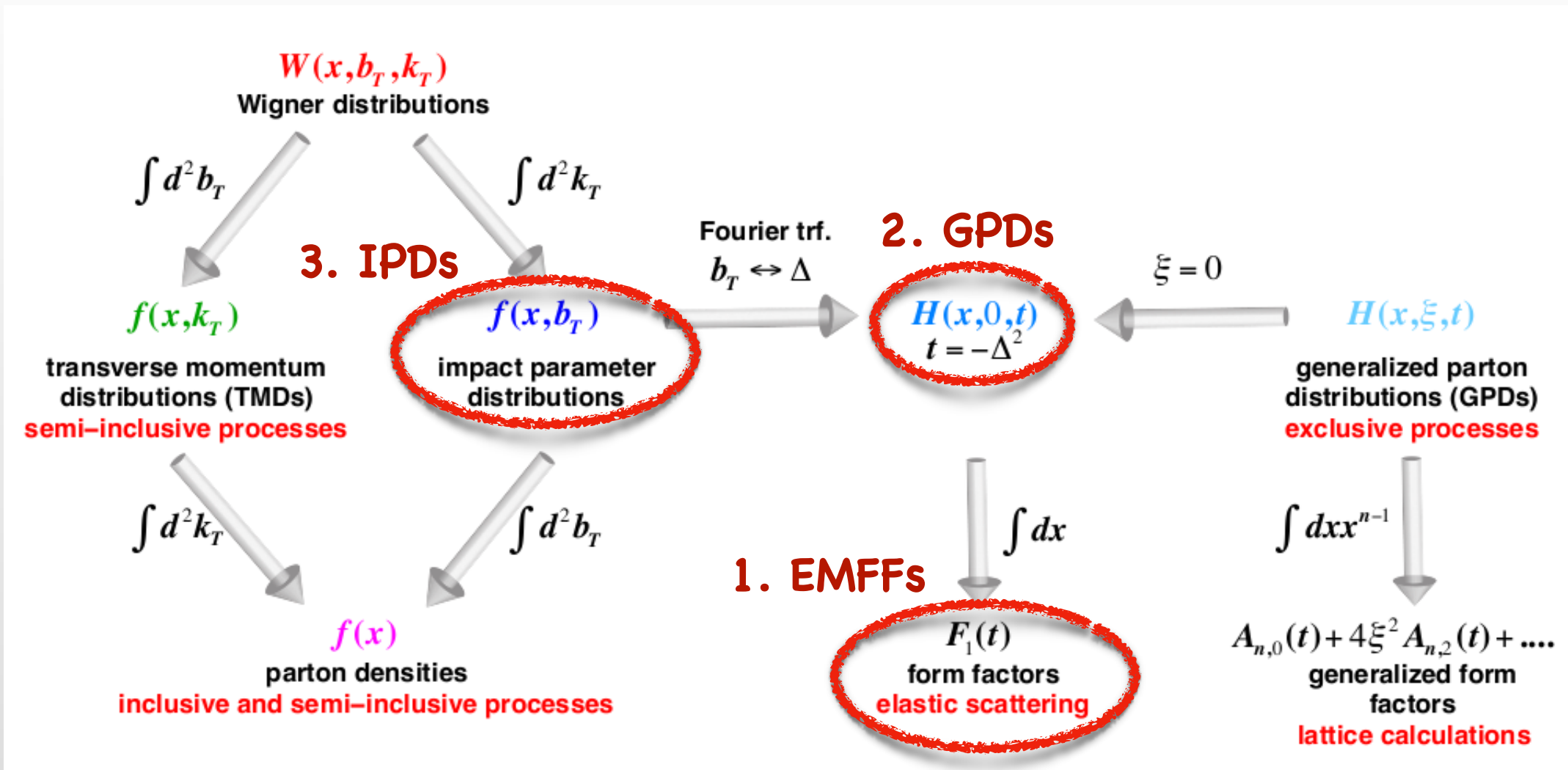
Partons



Wigner Distributions



Our topics



From 1D Size to 3D Tomography

1D EMFFs: Global structure

- 📌 Low Q^2 : How big is the meson?
- 📌 High Q^2 : Hadronic \Rightarrow Partonic
Non-perturbative \Rightarrow Perturbative

3D GPDs: Internal partons

- 📌 Where are the quarks inside?
- 📌 3D impact-parameter distributions

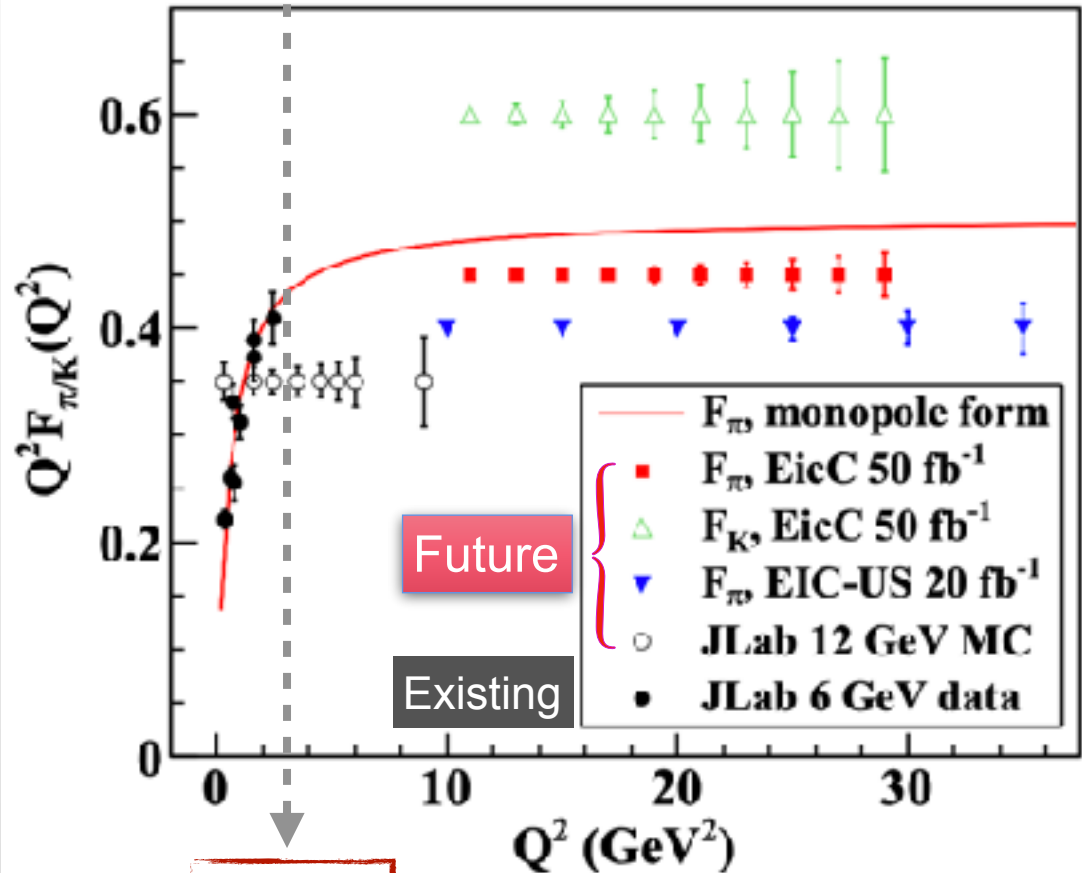
Providing critical benchmarks for the future experimental facilities

Approches

- 🌐 Experiment: indirect extraction, high cost, limited coverage
- ★ **Lattice QCD: non-perturbative, first principle**
- ☆ Perturbative QCD: not reliable at lower energy scales
- ☆ Factorization Framework: relies on non-perturbative inputs
- ☆ Other methods: model assumptions
e.g. Dyson-Schwinger equation (DSE), vector meson dominance (VMD) model, ...

Current Landscape and Future Reach

Front. Phys. 16 (2021) 64701



3 GeV²

Momentum transfer $Q^2 = -t$

Meson research is very limited

EPJA 48 (2012) 187 JPG 48 (2021) 075106 arXiv: 2102.09222

Experiment: JLab12, EIC, EicC ...

Gao et al., PRD 96 (2017) 034024

Effective theory: QCD sum rules, DSE ...

Lattice QCD:

- State-of-the-art:

PRD 96 (2017) 114509 ETMC, PRD 105 (2022) 054502

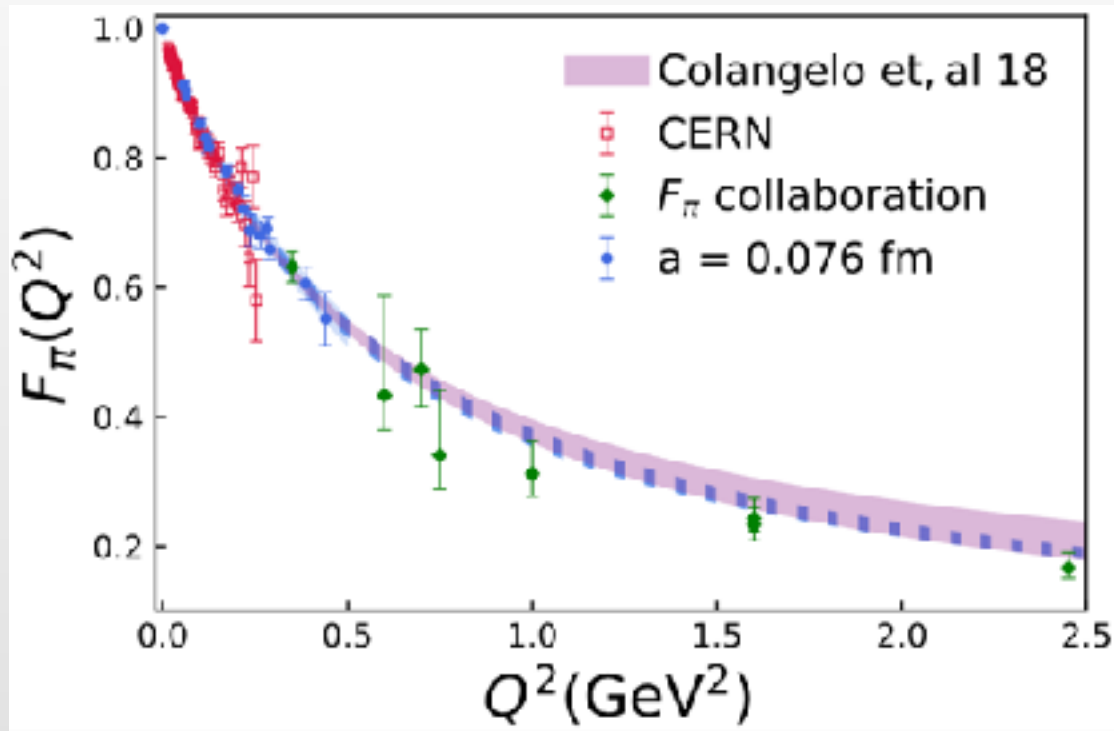
$$Q^2 \leq 6 \text{ (pion)}, 3 \text{ (kaon)} \text{ GeV}^2$$

- This work:

$$Q^2 \text{ up to } 10 \text{ (pion)}, 28 \text{ (kaon)} \text{ GeV}^2$$

The Gap at Higher Q^2

Low Q^2 : Good agreement



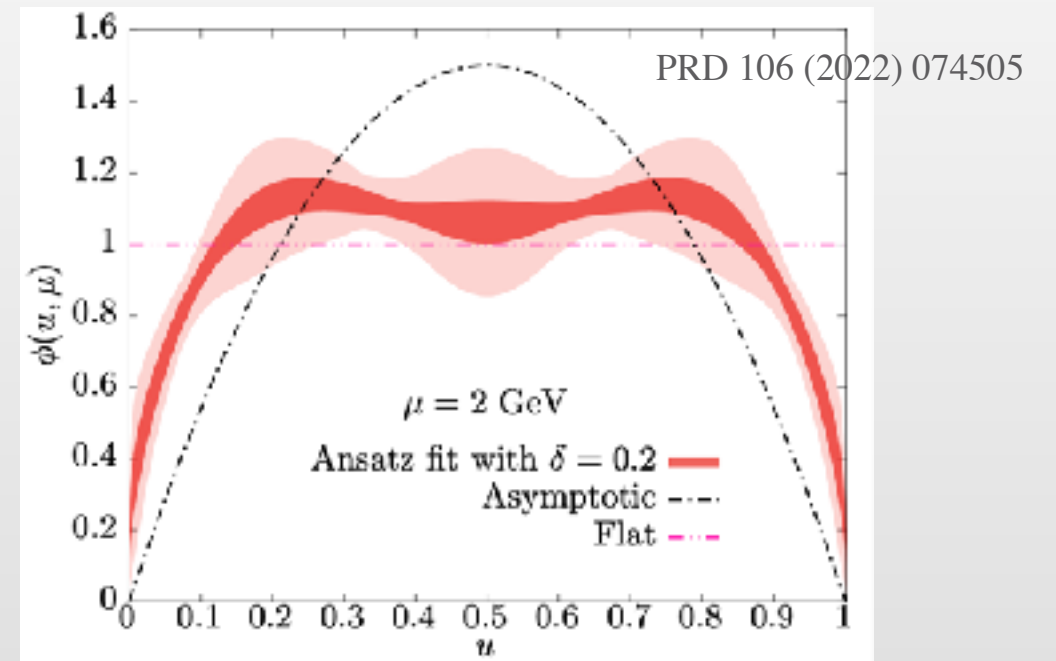
PRD 104 (2021) 114515



Larger Q^2

High Q^2 : Factorization framework

$$F(Q^2) = \int \int dx dy \underbrace{\Phi^*(y, \mu_F^2)}_{\text{Distribution amplitude}} \underbrace{T_H(x, y, Q^2, \mu_R^2, \mu_F^2)}_{\text{Hard-process kernel}} \Phi(x, \mu_F^2)$$



Test the factorization framework



The Challenge of Extracting 3D Structure

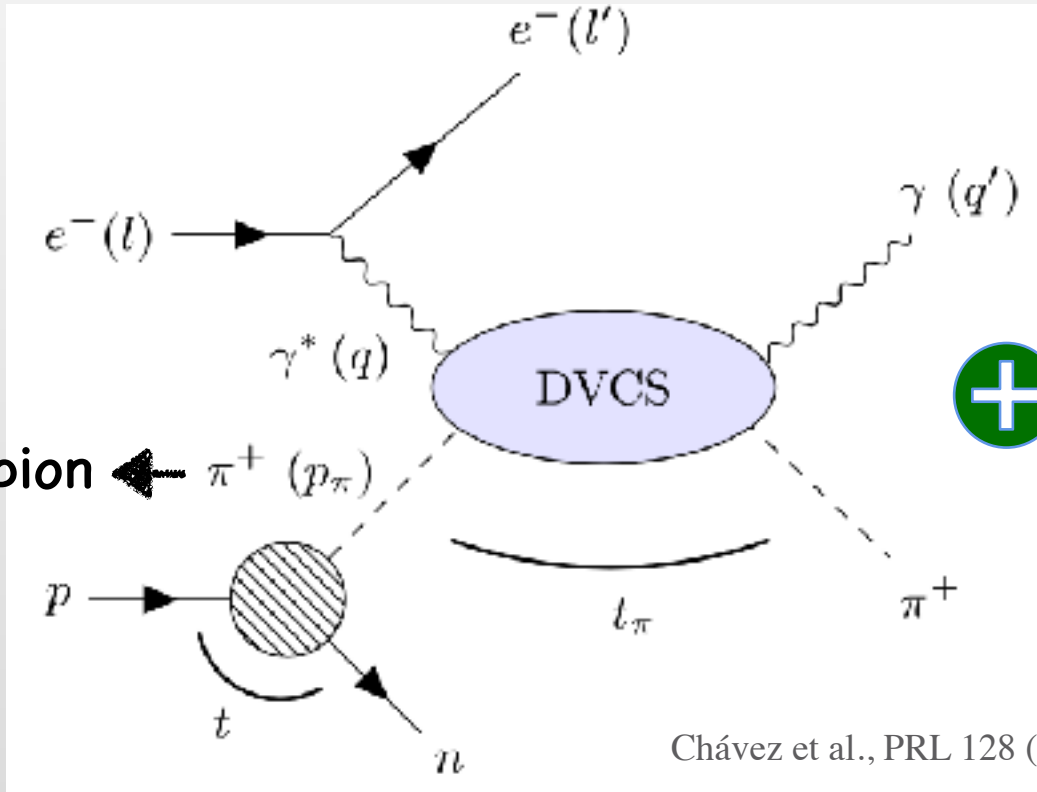
1D

- Form Factors (FFs)
- Parton Distribution Functions (PDFs)



3D

Generalized Distribution Functions (GPDs)



Produce the pion

+ Models

Chávez et al., PRL 128 (2022) 202501

More Difficult

Lattice QCD !

CONTENTS

- 1 Background and Motivation
- 2 Lattice QCD Methodology
- 3 Hadron Structure:
 - ☆ Electromagnetic Form Factors (EMFFs)
 - Based on *Phys. Rev. Lett.* 133 (2024) 18, 181902
 - ☆ Generalized Parton Distributions (GPDs)
 - Based on *JHEP*, 02 (2025) 056
- 4 Conclusion

Lattice QCD

- Discretizing spacetime: $N_s^3 \times N_t$
- From first principles \Leftrightarrow From Lagrangian

Lagrangian $\mathcal{L}_{\text{QCD}} \rightarrow$ action $S \rightarrow$

$$\langle O \rangle = \frac{1}{Z} \int \mathcal{D}A \mathcal{D}\bar{\psi} \mathcal{D}\psi O e^{-S}$$

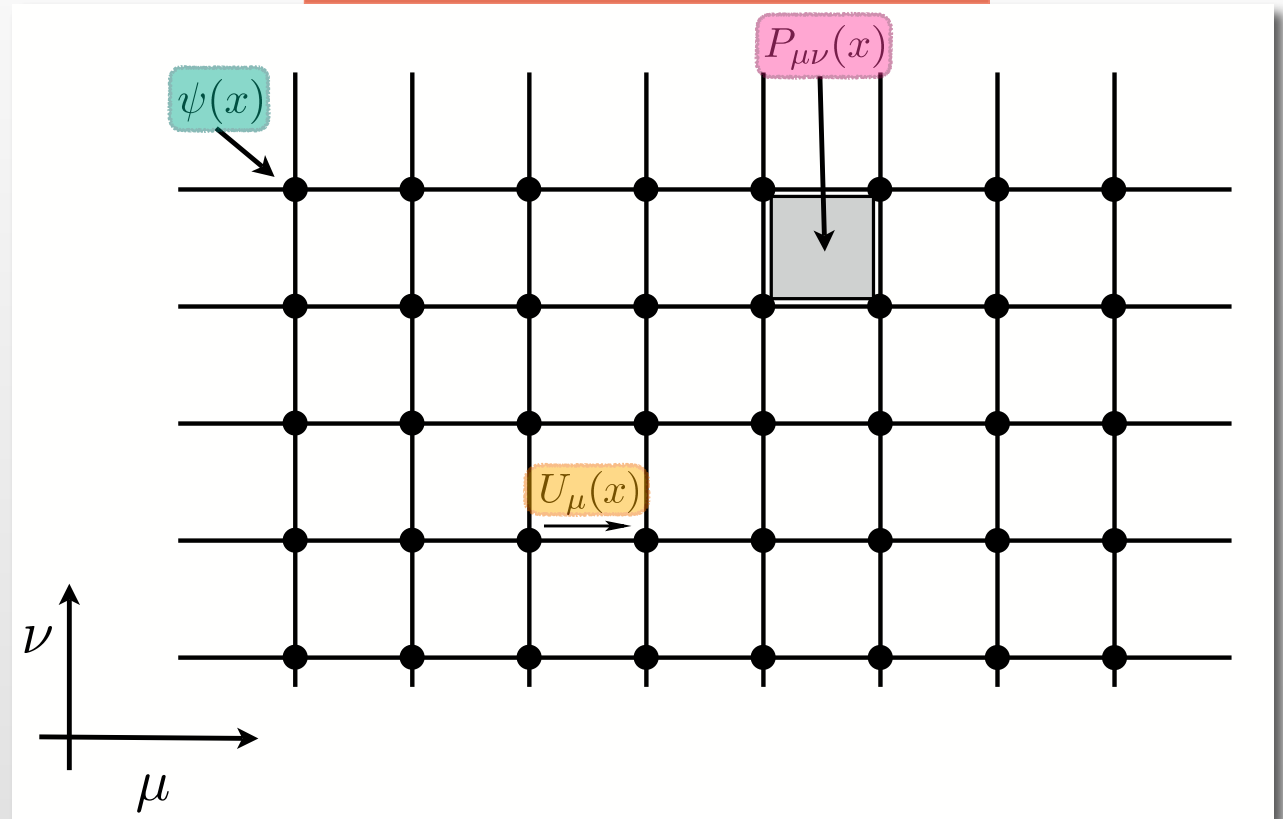
Gluon fields Quark fields

Gauge invariance: $A \rightarrow U \rightarrow P$

Link variable $U_\mu(x) = \exp\left(ig_s a A_\mu(x)\right)$

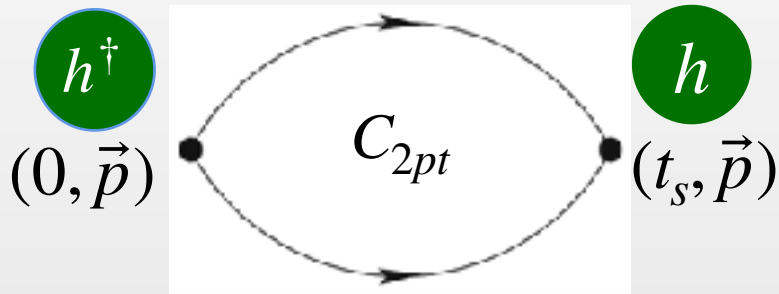
Plaquette $P_{\mu\nu}(x) = U_\mu(x)U_\nu(x + \hat{\mu})U_\mu^\dagger(x + \hat{\nu})U_\nu^\dagger(x)$

Simplified 2D lattice



Lattice QCD

$$\langle O \rangle = \frac{1}{Z} \int \mathcal{D}A \mathcal{D}\bar{\psi} \mathcal{D}\psi O e^{-S}$$

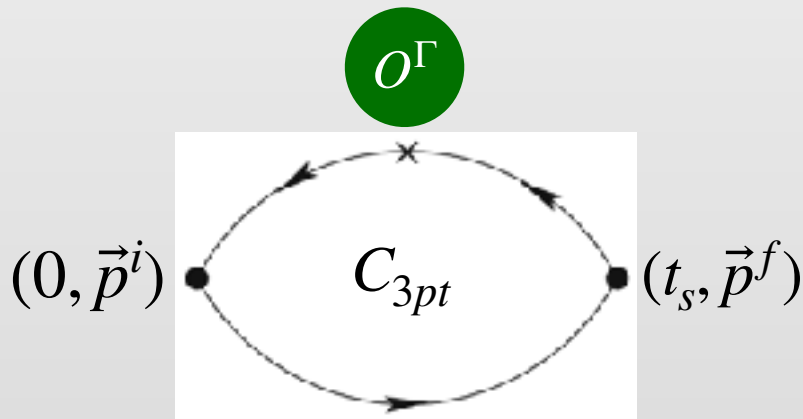


$$C_{2pt}(\mathbf{P}, t_s) = \langle h(\mathbf{P}, t_s) h^\dagger(\mathbf{P}, 0) \rangle$$



$$O^\Gamma(\Delta, \tau, z) = \sum_y e^{-i\Delta \cdot y} \bar{\psi}(y, \tau) \Gamma \mathcal{W}(z) \psi(y + z, \tau)$$

$$\mathbf{P}^f = \mathbf{P}^i + \Delta$$



$$C_{3pt}^\Gamma(\mathbf{P}^f, t_s, \Delta, \tau, z) = \langle h(\mathbf{P}^f, t_s) O^\Gamma(\Delta, \tau, z) h^\dagger(\mathbf{P}^i, 0) \rangle$$

Lattice QCD

$$\left\{ \begin{array}{l}
 C_{2pt}(t_s) = \sum_{k=0}^{N_{\text{state}}-1} A_k \left[e^{-E_k t_s} + e^{-E_k(aN_t - t_s)} \right] \xrightarrow{\text{Fit with } N_{\text{state}} = 2} E_0, E_1; A_0, A_1 \\
 \\
 C_{3pt}^\Gamma(\mathbf{P}^f, t_s, \Delta, \tau, z) = \sum_{n,k=0}^{N_{\text{state}}-1} \underbrace{\langle 0 | \hat{h}(\mathbf{P}^f, t_s) | n \rangle}_{A_n} \underbrace{\langle k | \hat{h}^\dagger(\mathbf{P}^i, 0) | 0 \rangle}_{A_k} e^{-(\Delta E_k^i - \Delta E_n^f)\tau} e^{-\Delta E_n^f t_s} \langle n | \hat{O}^\Gamma(\Delta, \tau, z) | k \rangle \\
 \hspace{15em} \text{Can be canceled by } C_{2pt} \hspace{15em} \downarrow n = k = 0 \\
 \hspace{15em} M^B
 \end{array} \right.$$

$\xrightarrow{\text{green arrow}} R^{fi} \sim C_{3pt} / C_{2pt} \xrightarrow{t_s \rightarrow \infty} \text{Bare matrix element } M^B \xrightarrow[\text{local}]{z=0} \text{Bare form factor } F^B$

Lattice data (Euclidean space) \Rightarrow Physical observables (Minkowski space) ?

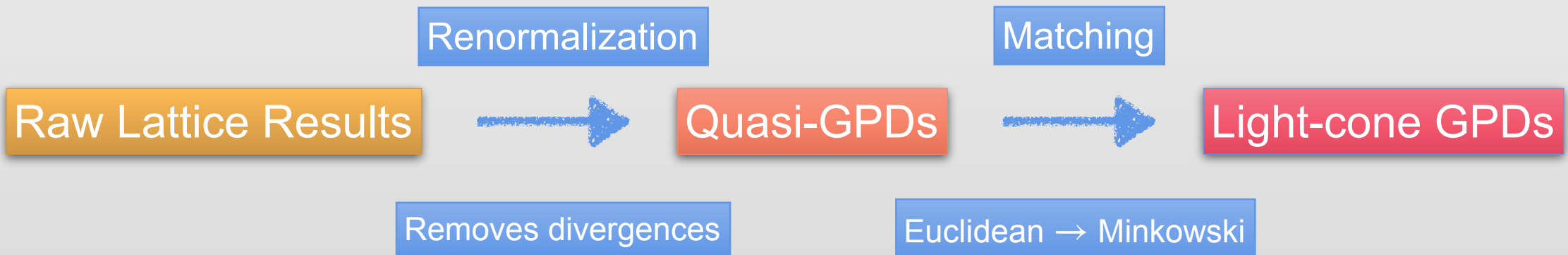
From Lattice to Physical World

Local Operator

- EMFFs
- Wilson line length: $z = 0$
- No anomalous dimension
- Divided by $1/Z_V = F^B(0)$

Non-local Operator

- GPDs
- Quarks separated by a Wilson line
- Suffer from various divergences
- Renormalization + Matching



CONTENTS

- 1 Background and Motivation
- 2 Lattice QCD Methodology
- 3 Hadron Structure:
 - ★ Electromagnetic Form Factors (EMFFs)
 - Based on ***Phys. Rev. Lett.*** 133 (2024) 18, 181902
 - ☆ Generalized Parton Distributions (GPDs)
 - Based on ***JHEP***, 02 (2025) 056
- 4 Conclusion

EMFFs: Lattice Setup

📍 Lattice size: $N_s^3 \times N_t = 64^3 \times 64$

📍 Lattice spacing: $a = 0.076$ & 0.04 fm for kaon, $a = 0.076$ fm for pion

📍 Sea quark: Highly Improved Staggered Quark (HISQ) action

Valence quark: Wilson-Clover action

⇒ **at the physical point**

• State-of-the-art:

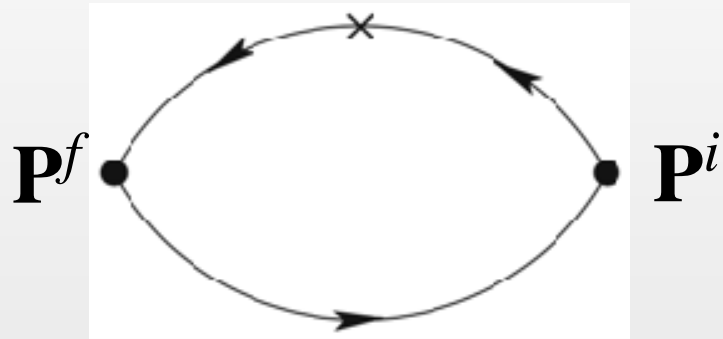
$Q^2 \leq 6$ (pion), 3 (kaon) GeV^2

• **This work:**

Q^2 up to 10 (pion), 28 (kaon) GeV^2

EMFFs: Techniques to High Q^2

Previous studies:

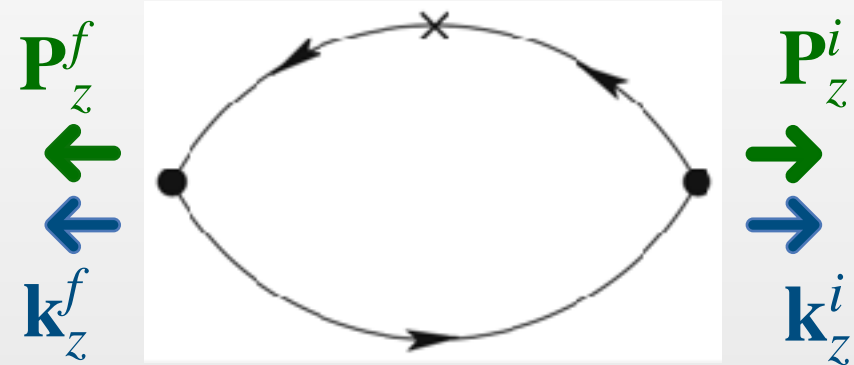


- ▶ Fix \mathbf{P}_z , only vary \mathbf{P}_\perp
- ▶ Fix \mathbf{P}^f , only vary \mathbf{P}^i



Limited Q^2

This work:



- ▶ Vary \mathbf{P}^i & \mathbf{P}^f (\mathbf{P}_\perp & \mathbf{P}_z)

- ▶ Momentum smearing: $\zeta = \frac{\mathbf{k}_z^i}{\mathbf{p}_z^i} = \frac{\mathbf{k}_z^f}{\mathbf{p}_z^f}$



Higher Q^2

EMFFs: $C_{2\text{pt}}$

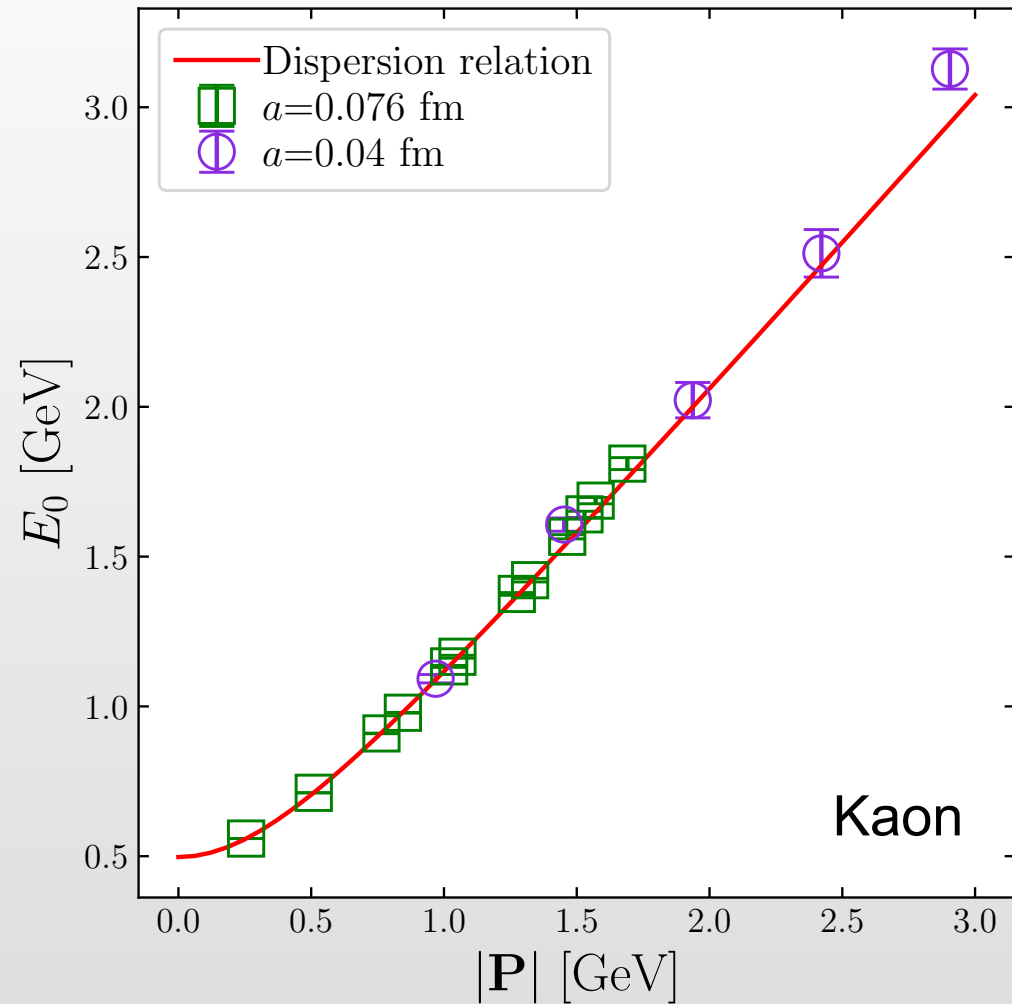
🔍 Extract E & A from $C_{2\text{pt}}$

$$C_{2\text{pt}}(t_s) = \sum_{k=0}^{N_{\text{state}}-1} A_k \left[e^{-E_k t_s} + e^{-E_k(aN_t - t_s)} \right]$$



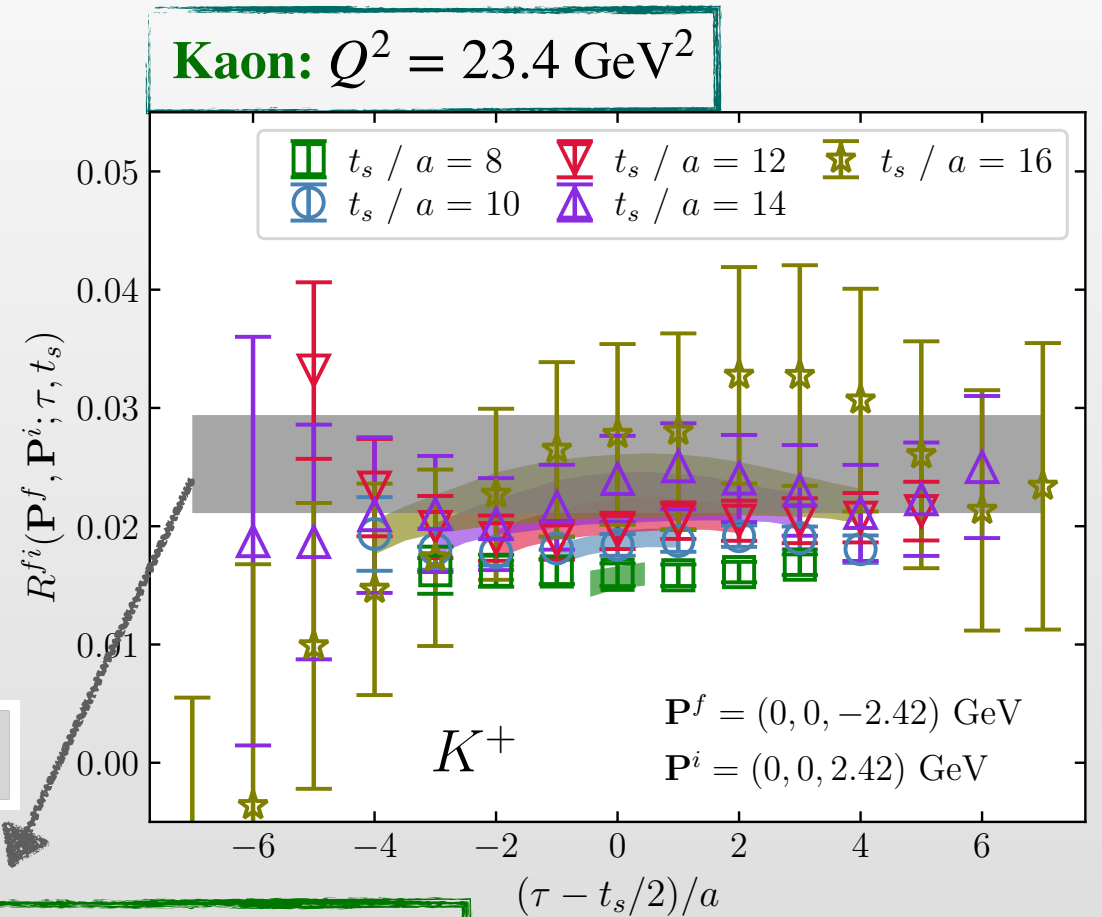
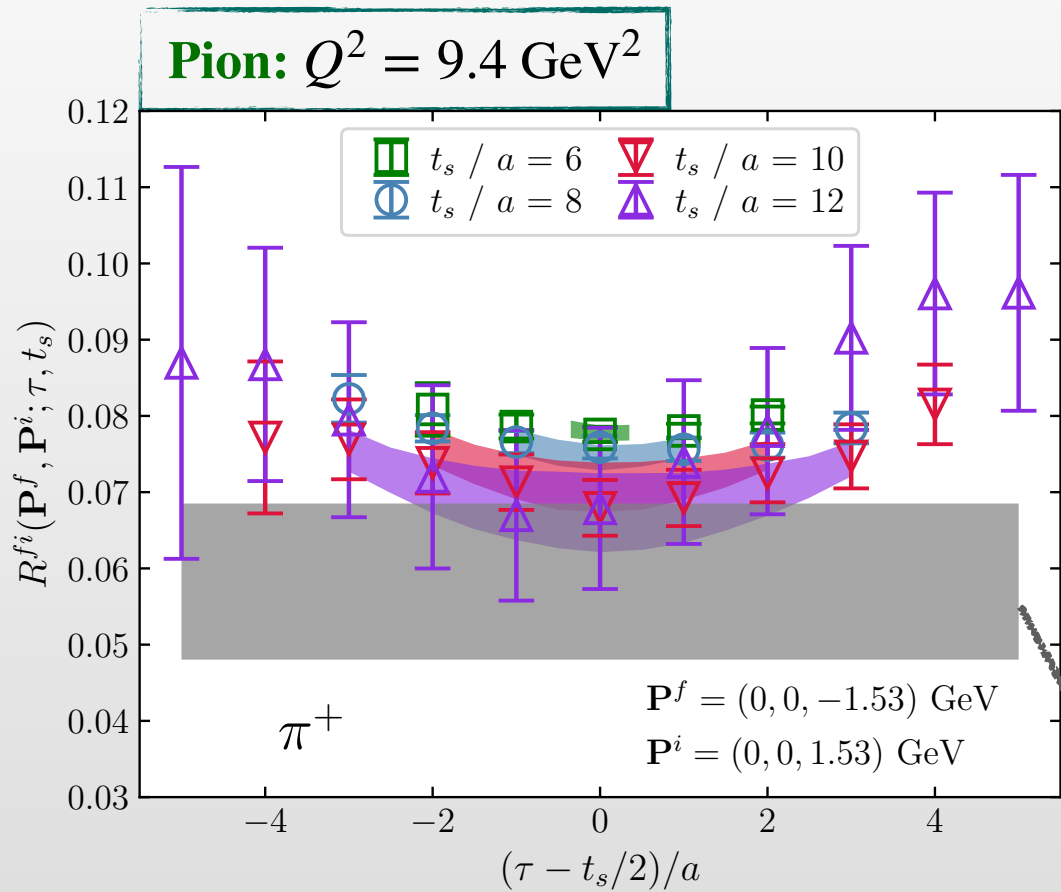
Fit with $N_{\text{state}} = 2$

$E_0, E_1; A_0, A_1$



EMFFs: Bare FF F^B

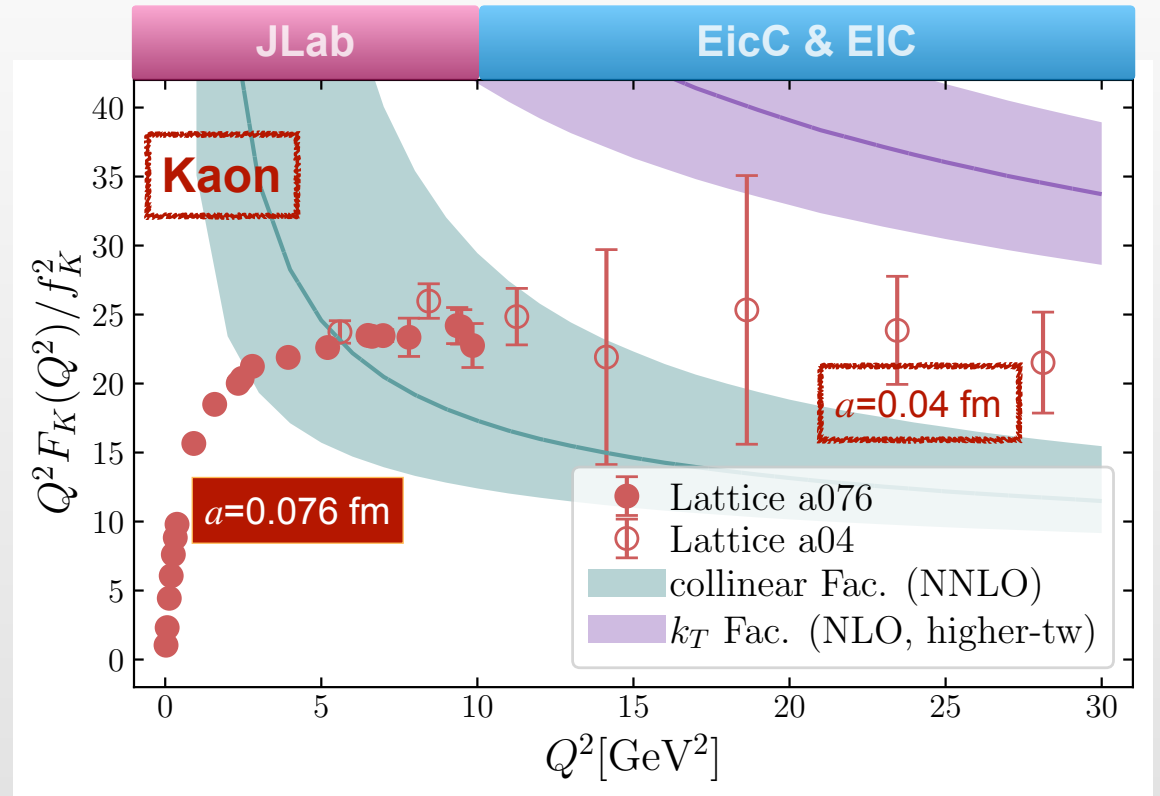
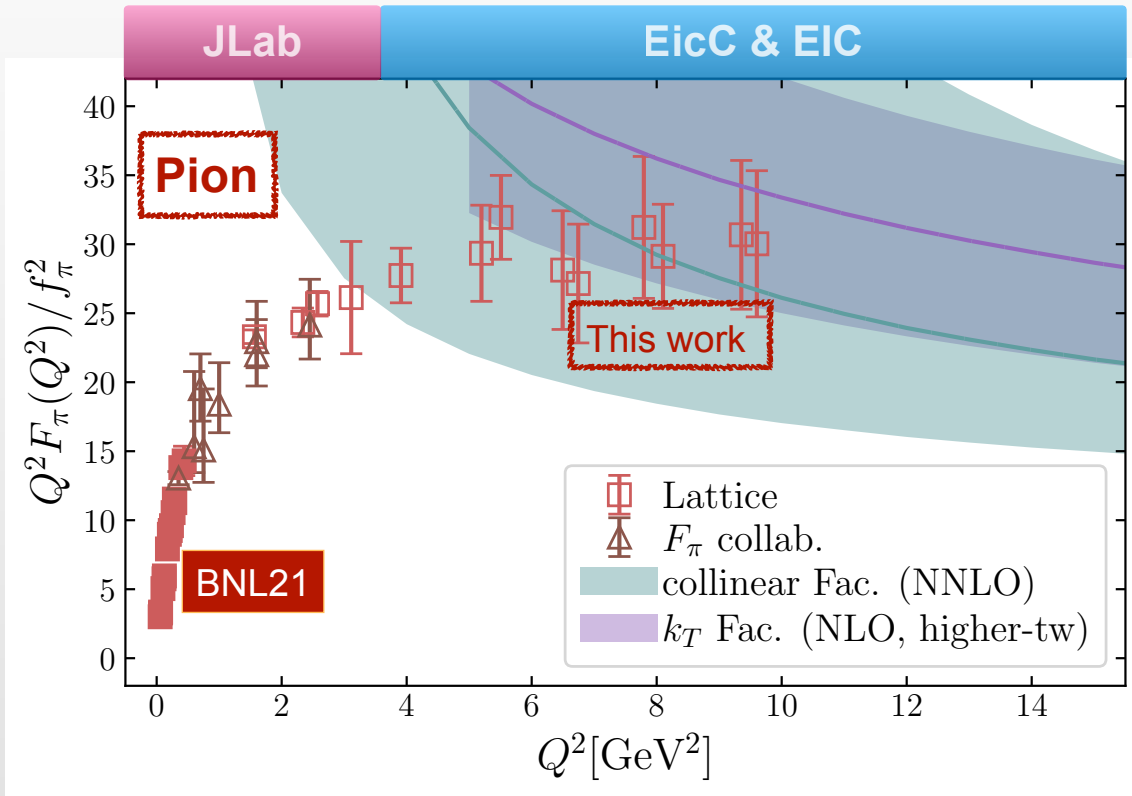
📍 Extract F^B from $R^{fi} \sim C_{3pt}/C_{2pt}$



$t_s \rightarrow \infty$

Bare Form factor $F^B \times Z_V^{-1} = F(Q^2)$

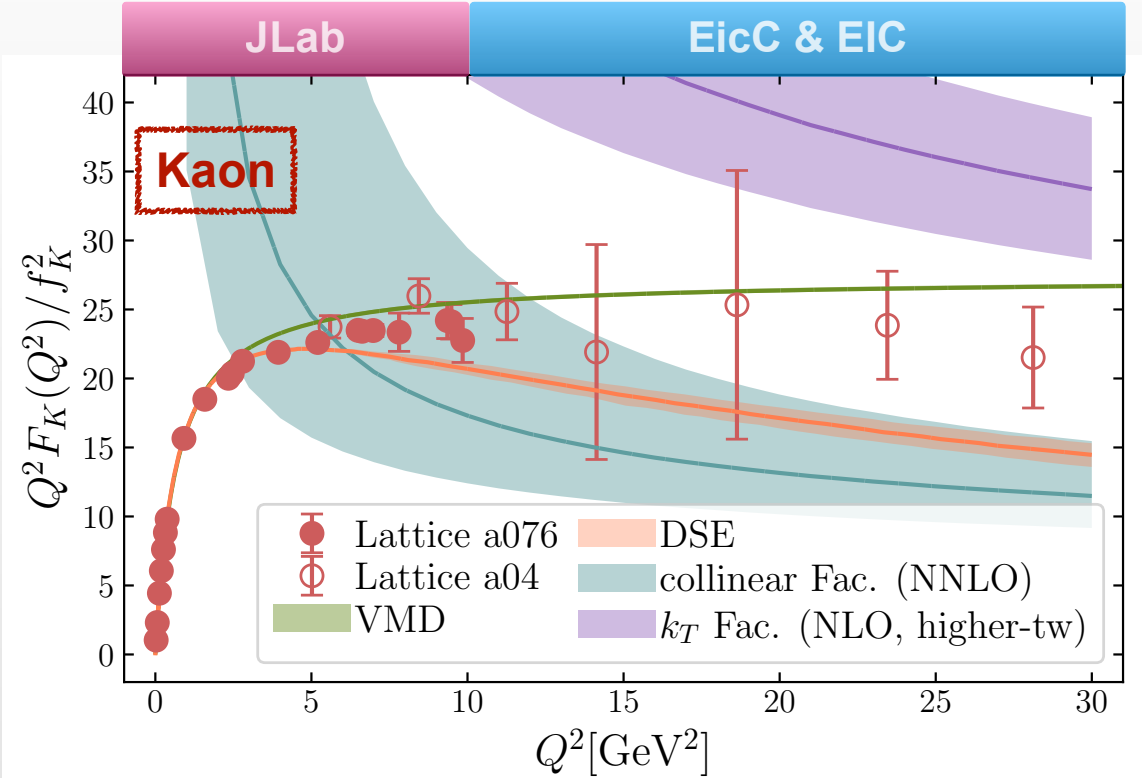
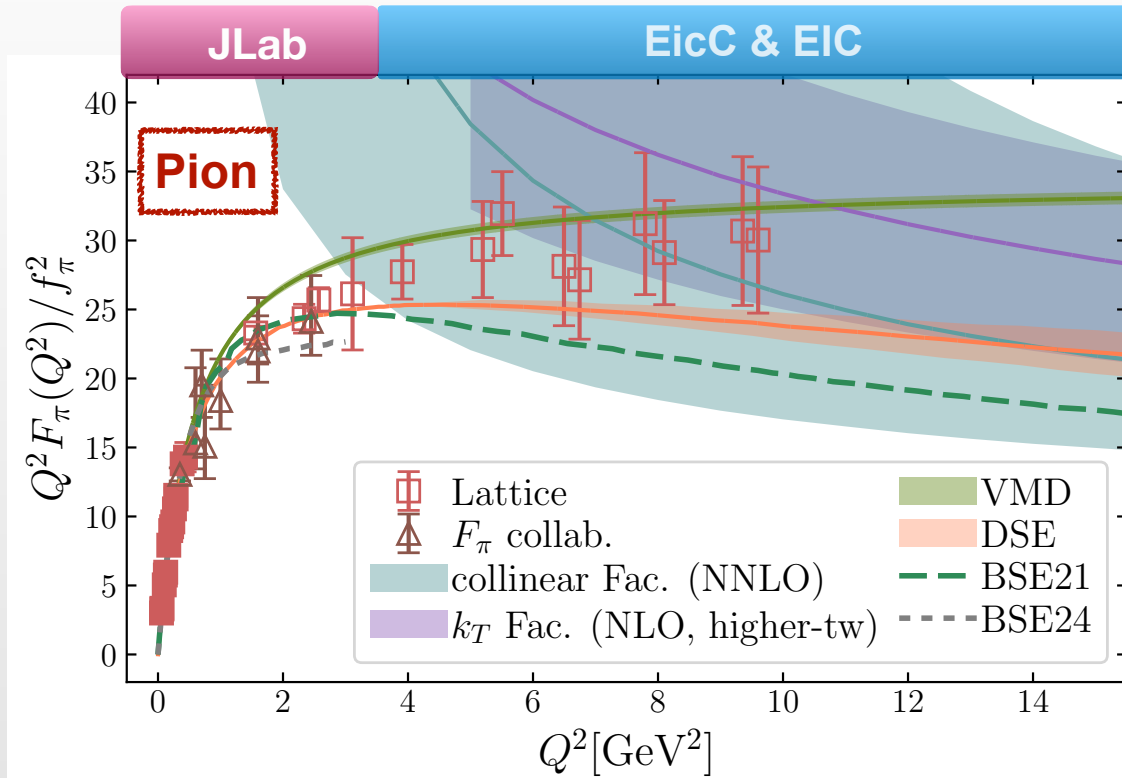
$$Q^2 F(Q^2)/f^2 \xrightarrow{Q^2 \rightarrow \infty} \text{Constant}$$



$$F(Q^2) = \int \int dx dy \underbrace{\Phi^*(y, \mu_F^2)}_{\text{Distribution amplitude}} \underbrace{T_H(x, y, Q^2, \mu_R^2, \mu_F^2)}_{\text{Hard-process kernel}} \Phi(x, \mu_F^2)$$

Lattice (BNL21): Gao et al., PRD 104 (2021) 114515
 F_π collaboration: Huber et al., PRC 78 (2008) 045203
 k_T factorization: Cheng, PRD 100 (2019) 013007
 pion: Chai et al., EPJC 83 (2023) 556;
 kaon: in preparation -> Chai and Cheng, JHEP 06 (2025) 229
 T_H in the collinear factorization: Chen et al., PRL 132 (2024) 201901
 DA in the collinear factorization: Cloët et al., arXiv:2407.00206

EMFFs



• **VMD**: Vector Meson Dominance

• **DSE**: Dyson-Schwinger Equation

• **BSE**: Bethe-Salpeter Equation

Lattice (BNL21): Gao et al., PRD 104 (2021) 114515
 F_π collaboration: Huber et al., PRC 78 (2008) 045203
 k_T factorization: Cheng, PRD 100 (2019) 013007
 pion: Chai et al., EPJC 83 (2023) 556;
 kaon: in preparation -> Chai and Cheng, JHEP 06 (2025) 229
 T_H in the collinear factorization: Chen et al., PRL 132 (2024) 201901
 DA in the collinear factorization: Cloët et al., arXiv:2407.00206
 DSE (Dyson-Schwinger equation): Yao et al., PLB 855 (2024) 138823
 BSE21 (Bethe-Salpeter equation): Ydrefors et al., PLB 820 (2021) 136494
 BSE24: Jia and Cloët, arXiv:2402.00285

CONTENTS

- 1 Background and Motivation
- 2 Lattice QCD Methodology
- 3 Hadron Structure:
 - ☆ Electromagnetic Form Factors (EMFFs)
 - Based on *Phys. Rev. Lett.* 133 (2024) 18, 181902
 - ★ Generalized Parton Distributions (GPDs)
 - Based on *JHEP*, 02 (2025) 056
- 4 Conclusion

GPDs: Lattice Setup & Techniques

- 📌 $N_s^3 \times N_t = 64^3 \times 64$, $a = 0.04$ fm
- 📌 HISQ action + Wilson-Clover action $\Rightarrow m_\pi^{\text{val}} = 0.3$ GeV
- 📌 Using momentum smearing to enhance the signal
- 📌 Momentum transfer Q^2 : $0 \sim 1.7$ GeV²
- 📌 Zero skewness $\xi = 0$ ($\Delta^z = 0$)
- 📌 **Frame-independent approach: save computational cost**

Bhattacharya et al., PRD 106 (2022) 114512

GPDs: Frame-independent Approach

- Lorentz-invariant amplitudes A_i 's (frame-independent)

$$M^\mu(P^m u, z^\mu, \Delta^\mu) = \bar{P}^\mu A_1 + m^2 z^\mu A_2 + \Delta^\mu A_3, \quad \bar{P}^\mu = (p_f^\mu + p_i^\mu)/2, \quad \Delta^\mu = p_f^\mu - p_i^\mu.$$

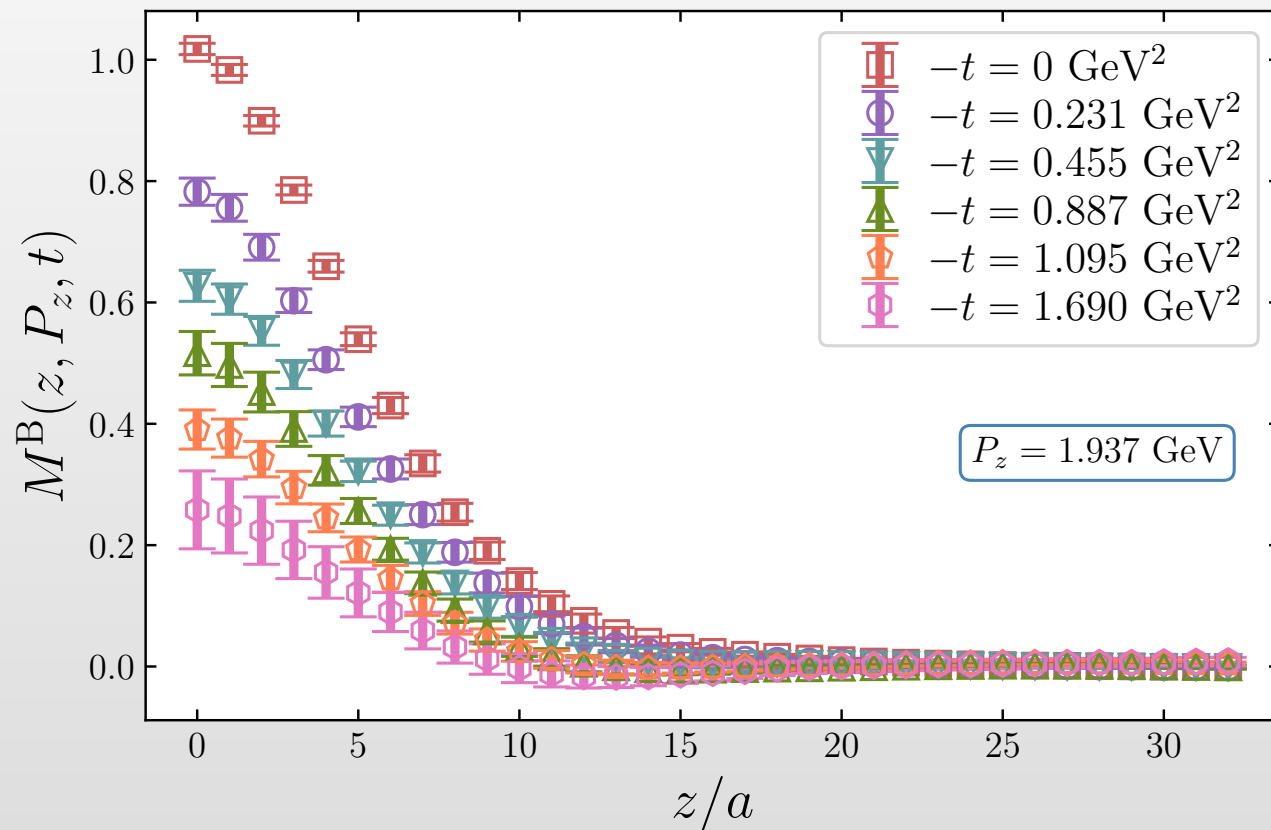
- Lorentz-invariant quasi-GPD \tilde{H}_{LI}

$$\tilde{H}_{\text{LI}}(z \cdot P, z \cdot \Delta, \Delta^2, z^2) = A_1 + \frac{z \cdot \Delta}{z \cdot \bar{P}} A_3 \quad \xrightarrow{A_3(z \cdot \Delta = 0) = 0} \quad \boxed{\tilde{H}_{\text{LI}} = A_1 = M^\mu / \bar{P}^\mu \equiv M^B}$$

Bare Matrix Elements

GPDs: Bare Matrix Elements

 Largest momentum: $P_z = 1.937$ GeV



$$\left. \begin{array}{l} z \uparrow \\ -t \uparrow \end{array} \right\} M^B \downarrow$$

Renormalization
 \longrightarrow
Fourier Transform

Quasi-GPDs
 $\tilde{H}(x, P_z, t)$

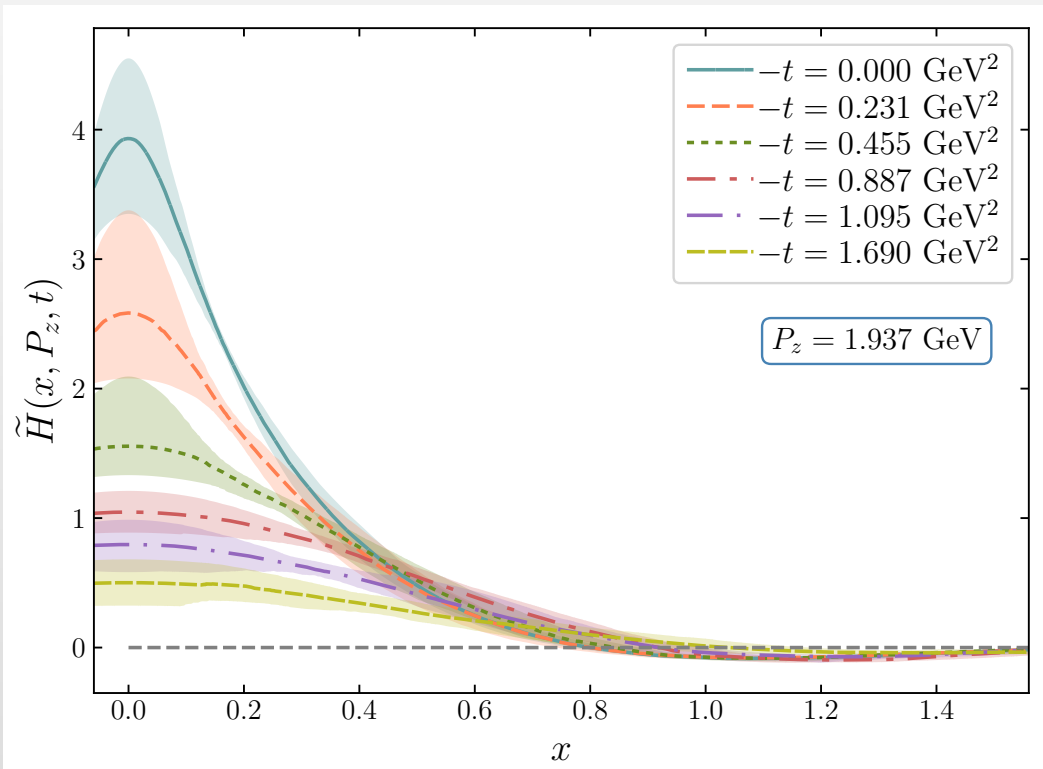
GPDs: Quasi-GPDs \tilde{H}

📌 Renormalization:

Ji et al., NPB 964 (2021) 115311

☆ RI/MOM, ratio schemes (short distance)

★ Hybrid scheme (short & long distance)



$$M^R(z, z_S; P_z, t) = \begin{cases} |z| \leq |z_S| : \frac{M^B(z, P_z, t)}{M^B(z, 0, 0)}, \text{ Ratio scheme} \\ |z| > |z_S| : \frac{M^B(z, P_z, t)}{M^B(z_S, 0, 0)} e^{(\delta m + \bar{m}_0)|z - z_S|} . \end{cases}$$

📌 Fourier Transform:

$$\int \frac{d\lambda}{\pi} e^{ix\lambda} M^R(z, P_z, t) \Rightarrow \tilde{H}(x, P_z, t)$$

GPDs: Matching

 **Large Momentum Effective Theory (LaMET)** framework

LC GPDs

NNLO+LRR+RGR

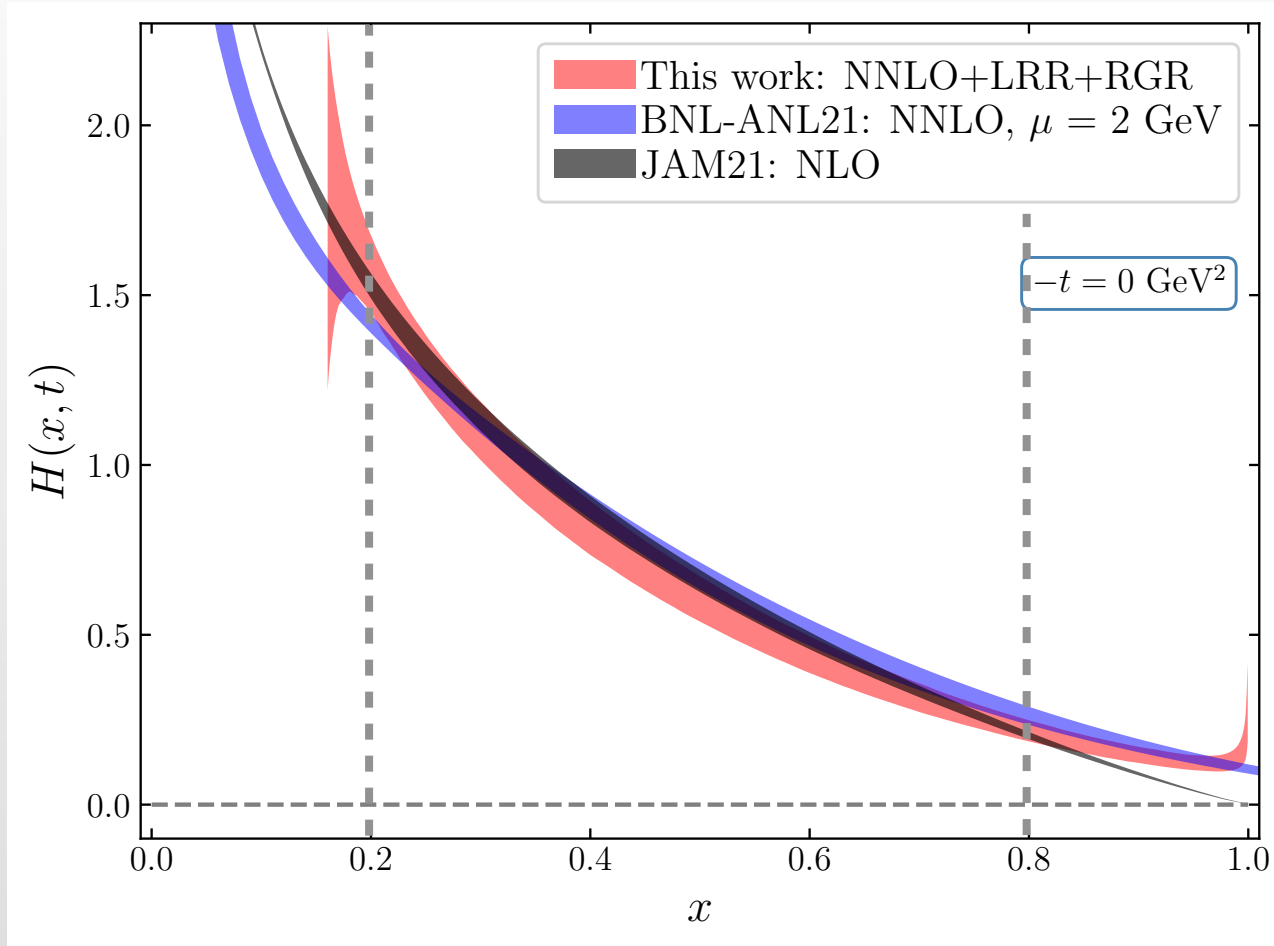
quasi-GPDs

$$H(x, t) = \int \frac{dk}{|k|} \int \frac{dy}{|y|} C_{\text{evo}}^{-1} \left(\frac{x}{k}, \frac{\mu}{\mu_0} \right) C^{-1} \left(\frac{k}{y}, \frac{\mu_0}{yP_z}, |y| \lambda_S \right) \tilde{H}(y, P_z, t, z_S, \mu_0) + \mathcal{O} \left(\frac{\Lambda_{\text{QCD}}^2}{(xP_z)^2}, \frac{\Lambda_{\text{QCD}}^2}{[(1-x)P_z]^2} \right)$$

- ▶ Next-to-next-to-leading order (NNLO) correction → More precise matching
- ▶ Leading-renormalon resummation (LRR) → Improve convergence of perturbation series
- ▶ Renormalization group resummation (RGR) → Improves reliability of matching at small x

Physical scale: $\mu_0 = 2\kappa e^{-\gamma_E} / |z|$, $\kappa = [1, \sqrt{2}, 2]$ → Factorization scale: $\mu = 2 \text{ GeV}$.

GPDs: Light-cone (LC) PDFs



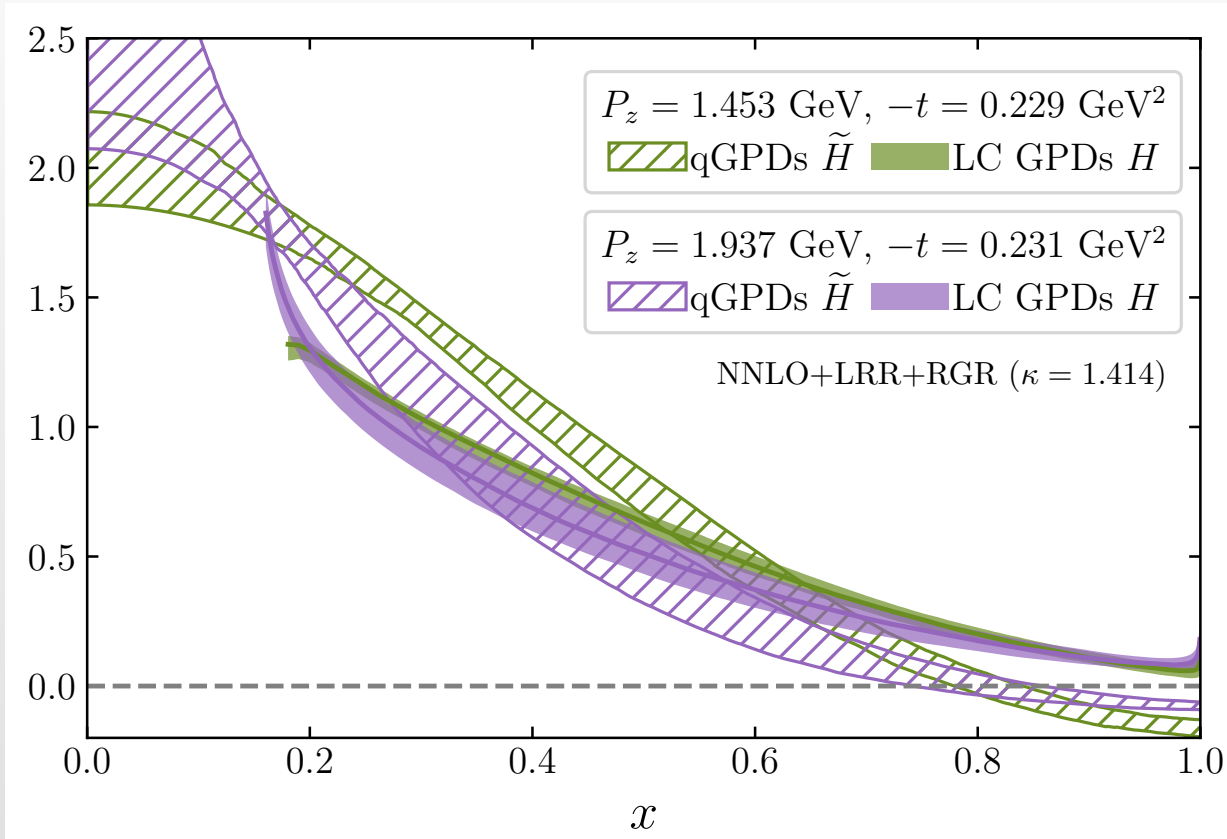
GPDs at $-t = 0 \text{ GeV}^2 \rightarrow$ PDFs

$0.2 < x < 0.8$: comparable with JAM21

Both ends of x :

LRR + RGR \rightarrow different with BNL-ANL21

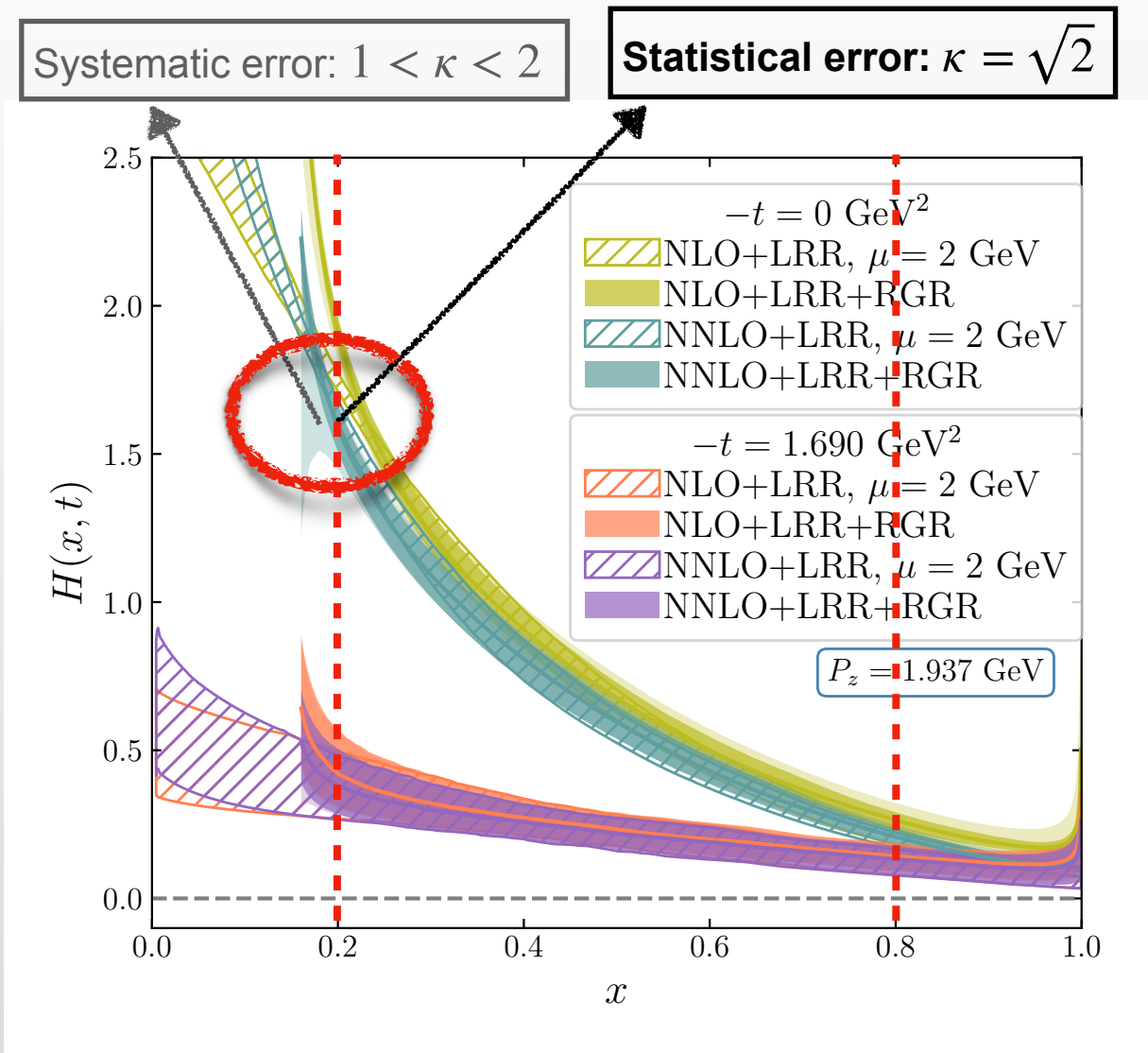
GPDs: Matching effect on P_z -dependence, q V.S. LC



Perturbation matching:

- Same data set, difference \rightarrow effect of perturbation matching
- Different data sets \rightarrow Reduce the P_z -dependence

LC GPDs: Scale & Order dependence



Scale dependence

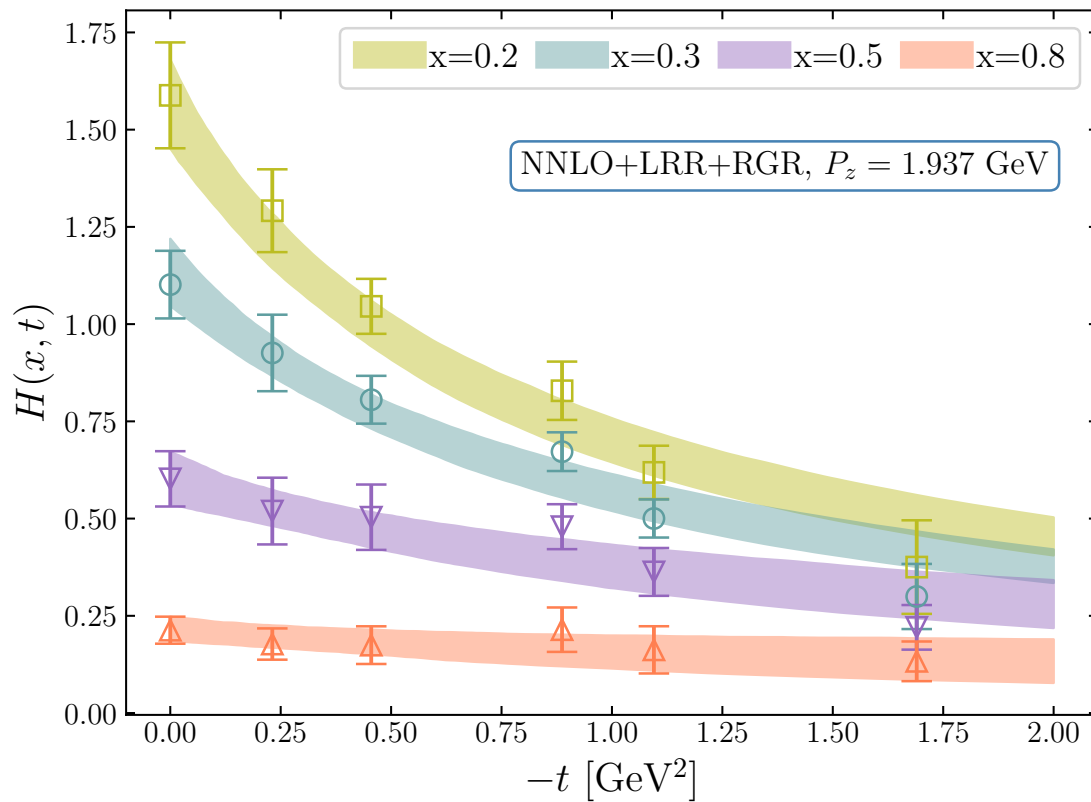
- More significant at small and large x
- Smaller at larger $-t$

Good convergence: NLO & NNLO

RGR:

- reliable x : 0.2 - 0.8
- small x : perturbation theory breaks down
- large x : threshold logarithms in the future

LC GPDs: t -, x -dependence & IPDs



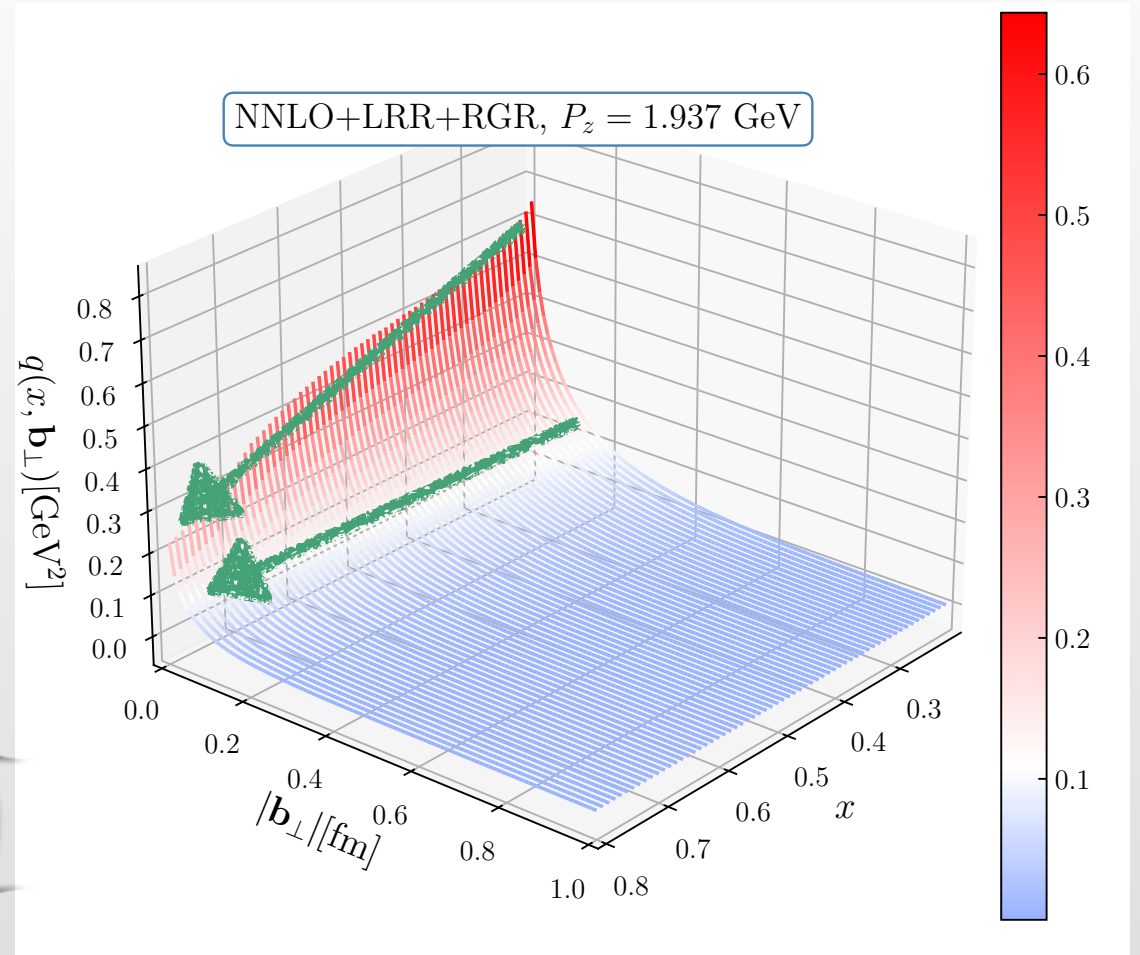
- Monopole model: $H(x, t) = \frac{H(x, 0)}{1 - t/M^2(x)}$ PDFs
- t -dependence becomes milder as x increases

LC GPDs \rightarrow IPDs

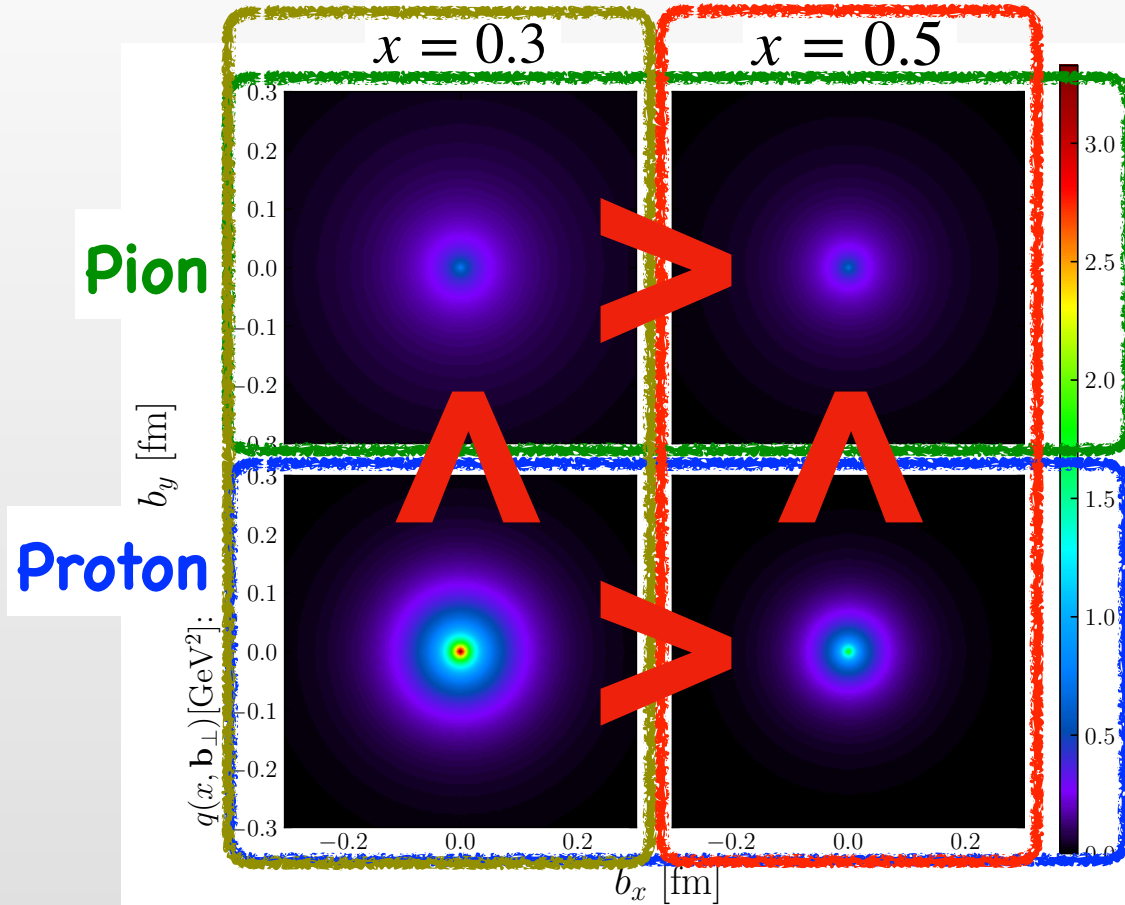
$$q(x, \mathbf{b}_\perp) = \int \frac{d^2\Delta_\perp}{(2\pi)^2} H(x, \xi = 0, \Delta_\perp^2) e^{i\mathbf{b}_\perp \cdot \Delta_\perp}$$

$x \uparrow$ $\left\{ \begin{array}{l} \text{Probability} \downarrow \\ \text{Distributions on } b_\perp \text{ become narrow} \end{array} \right.$

Quarks with higher x are more concentrated in the transverse space



IPDs: Pion v.s. Proton



- LC Proton GPDs [Cichy et al., arXiv:2304.14970]
- Distributions are more concentrated at larger x in the transverse space
- Quark distributions in the proton are broader than those of the pion

Conclusions

★ Pion and kaon EMFFs at the physical point

- 🎤 Q^2 up to 10 and 28 GeV^2 for the pion and kaon
- 🎤 Consistent with experimental results and collinear factorization predictions
- 🎤 Serve as benchmark QCD predictions for model-based studies and the future experimental measurements

★ Pion LC GPD at zero skewness

- 🎤 Improved perturbation matching with NNLO + LRR + RGR
- 🎤 P_z^- , t^- , x^- , scale and order dependence of the LC GPDs & IPDs
- 🎤 Provide the three-dimensional image of the pion structure

Thanks for your attention !